# DESIGN CRITERIA OF A THERMAL MASS FLOW SENSOR FOR AIRCRAFT AIR DATA APPLICATIONS

**Ribeiro, L. C.*; Souza*, R. A.; Oliveira, M. L.; Vieira, S. P. L.; Avelino, W. O.**, Oliveira, C. F. R.*; de Lima Monteiro, D. W.*, Torres, F. S.*, Hansen, R. M. O***.**

**OptMA Lab UFMG*, Labinfo Lab UFMG**, South Denmark University*****
**Department of Electrical Engineering, Universidade Federal de Minas Gerais (UFMG), Brazil**
**Email: lucas.dcribeiro@gmail.com**

**Keywords**: *Aerospace systems, Aircraft Navigation, Thermal Mass Flow Sensor, Microelectromechanical Systems, Air Data Systems.*

## Abstract

*The operating environment of aircraft air-data sensors is extremely aggressive with a wide temperature and humidity variation, suspension particles, icing and etc. The Pitot tube is widely used as air-data sensor on aircrafts, which has had many operational issues reported in the past decades due to ice-crystal obstruction of its aperture. The Microelectromechanical Systems (MEMS) technology associated with Thermal Mass Flow Sensors (TMFS) can establish a reformulation on air-data system instrumentation, since it is possible to create micro heaters and thermal sensors on the same substrate without moving parts, simplifying the operational requirements compliant to the aeronautics specifications. Exploring the simplicity and robustness of MEMS technology, a TMFS is herein designed according to criteria that meet aeronautic performance requirements, selecting adequate dimensions of the various structures in the sensor and materials compatible with semiconductor micromachining processes. This paper also presents the numerical results of the interaction of a thermal mass flowing through the integrated heater element of the sensor.*

## 1 INTRODUCTION

IR Data Systems (ADS) are designed to provide information about the aircraft surrounding air properties to the aircraft systems. These include air pressure, temperature, density and viscosity as well as the speed of sound at the flight altitude, aircraft angles of attack and sideslip, true air speed and rate of climb [1, 2]. Typically, Pitot tubes and static pressure sensors are used to convert the airflow information into indications to the cockpit for flight crew usage during aircraft navigation, being the raw signals processed and digitally provided by the Air Data Computers (ADC) [2]. Additionally, the ADS data supplies very critical information to other aircraft systems and a safety assessment is generally performed, imposing at design level, an adequate and independent level of redundancy in the ADS architecture defining a robust logic for failure management [3, 4].

Every component embedded in the aircraft shall be qualified to operate in compliance with its respective operational zone and a series of technical assessments are performed during the aircraft design process helping to define the criticality level that will drive the system design [4, 5]. Once the system criticality level and their components operational zone are defined, the environment qualification levels can be set. The standard normally used by the aeronautical industry as reference is the DO-160 (latest revision is G) which defines a series of minimum environmental test conditions and applicable test procedures for airborne equipment qualification [6].

Even though the ADS system is critical to the aircraft navigation and is qualified to operate

in harsh environments, it is common to have incidents, or even accidents, involving the freezing of the Pitot-probe orifice despite its heating capabilities. Once ice crystals start to accumulate at the pitot-tube entrance, the data becomes noisy (or even lost) leading to ADC software to ignore the defective probe. This type of failure event caused the flight AF447, departing from Rio de Janeiro to Paris in 2009, to crash in the international waters on the Atlantic Ocean, near to TASIL point, leaving 228 people dead [7]. Additionally, at least two other incidents were reported on the past decades associated with the very same type of failure event. Fortunately, these airplanes had safely landed once the emergency condition was reported and the flight crew had taken the proper actions [8, 9].

In order to develop a more robust and fault tolerant ADS system, research efforts are focus on an alternative and viable solution for the Pitot sensors. Verbeek and Jentink [10] propose an optical ADS system that obtains the air-speed data from laser-based sensors. Results from a flight test indicate the system capability to operate in normal as well as in extreme conditions, including icing events. Lee et al [11] propose a piezoelectric sensor system based on the technology Microelectromechanical Systems (MEMS) that provides the static air pressure flow information around the aerial vehicle. Laboratory tests have proven the effectiveness of the proposed approach. Sturm et al [12] present a MEMS sensor applied as Thermal Mass Flow Sensor (TMFS). The sensor was tested in a wind tunnel with the intention to detect the airflow boundary layer separation and reattachment in an airfoil reporting successful results, for low speed operation.

It should be noted that MEMS technology is gaining attention from the general industry thanks to its size, repeatability, manufacturing costs and reliability. Therefore, several ADS system design companies are allocating resources on related research [13, 14].

This study intends to present the design criteria for a calorimetric thermal mass flow sensor (TMFS). In the next sections, the theory that support the sensor design is summarized and a detailed assessment will be presented as well as the CFD simulation results will be discussed.

## 2 MODELING FOR FLUID DYNAMICS

The Navier-Stokes equations are used in order to determine the velocity vector field which applies to a fluid, given particular initial conditions. These equations arise from the application of Newton's second law in combination with a fluid stress, due to its viscosity and compressibility effects, and the pressure term. For almost all real situations, it results in a system of nonlinear partial differential equations, which can be reduced to linear differential equations adopting certain simplifications. The Navier-Stokes equation is three-dimensional and can be written as a single vector equation using the indicial notation as follows [15]:

$$\rho \frac{D\boldsymbol{V}}{Dt} = \rho \boldsymbol{g} - \boldsymbol{\nabla} p + \boldsymbol{\nabla} \cdot \boldsymbol{\tau}'_{\boldsymbol{ij}} \qquad (1)$$

where V is the flow velocity vector, ρ is the fluid density, g is the body acceleration vector per unit mass acting on the continuum (i.e. gravity, inertial accelerations, electric field and so on), p is the pressure vector and $\boldsymbol{\nabla} \cdot \boldsymbol{\tau}'_{\mathbf{ij}}$ is the fluid viscous stress which represents the fluid deformation due to the strain forces.

The presented equation is the complete form of the Navier-Stokes equation that can be used to calculate the velocity vector field of any geometrical form subject to a flow. The phenomena associated with the intended application can be approximated to a flow on a flat plate, with its boundary layer development presented in Figure 1 and defined as the layer of fluid in the immediate vicinity of a bounding surface where the effects of viscosity are significant.

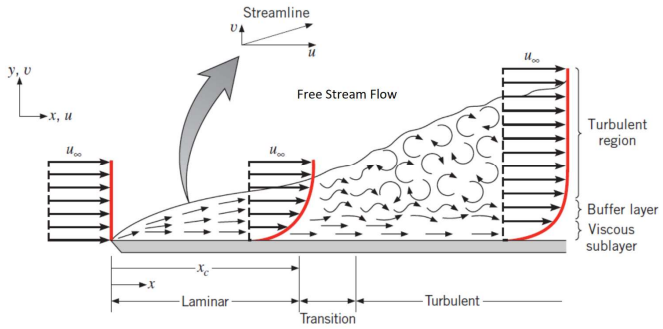


Fig. 1. Velocity boundary layer development on a flat plate [16].

To measure the flow velocity the proposed application will have a heat source transferring a constant amount of heat to the fluid which is transported away in the surface. The fluid velocity will be proportional to the loss of heat along the surface.

The relative longitudinal position of the heating and sensing elements of a TMFS on a flat plate determine the relation between heat transfer and flow speed. A measure of the flow behavior is given by the Reynolds Number, defining the distance where the flow will become turbulent and consequently demanding more heat to calculate the velocity. The flow transition point is then derived from the Reynolds Number equation, which represents the ratio of the inertia to viscous forces and described as [16]:

$$Re_x = \frac{\rho u_\infty x}{\mu} \quad (2)$$

where $u_\infty$ is the free stream velocity, $x$ is the point over the flat plate where it is desired to obtain the Reynolds Number and μ is the fluid viscosity. The transition from laminar to turbulent is obtained from Equation (2) based on the transition distance $x_c$, instead of $x$, defining the critical Reynolds Number which can vary from approximately $10^5$ to $3 \times 10^6$, depending on surface roughness and the turbulence level of the free stream and it is defined as the point where the sensor heating needs more power for speed reading.

To determine the amount of heat transfer needed to measure the desired speed it is necessary to solve the boundary layer equations for the flat plate, starting its development at the leading edge (x=0), obtaining the temperature profile. With that information the Nusselt number, a dimensionless parameter used to characterize the enhancement of the heat transfer due to convection, can be calculated. The Nusselt number is defined as the ratio of heat transferred from a surface to heat conducted away by the fluid being defined, for a flat plate with constant heat transfer average, as:

$$\overline{Nu_L} = 0.680 \cdot {Re_L}^{1/2} \cdot Pr^{1/3} \quad (3)$$

with $Pr$ known as the Prandtl Number, which is defined as the ratio of the kinematic viscosity to the thermal diffusivity and, therefore, a fluid property.

Then, with Reynolds and Nusselt Number in place it is possible to obtain the needed heat transfer rate average as:

$$\overline{h_L} = \overline{Nu_L} \cdot \kappa. \quad (4)$$

The electrical power that the heated element needs to generate is equal to the total heat transfer rate times the heating element area times the temperature difference between the heater and the fluid. It is expressed by:

$$q_{conv} = \overline{h_L} \cdot A_h \cdot (T_h - T_f) \quad (5)$$

where, $A_h$ is the heater surface area, $T_h$ is the heater temperature and $T_f$ is the fluid temperature.

The assumptions to calculate the dimensions of the calorimetric TMFS heater are: 1) the sensor is placed before the boundary layer transition point and, 2) the distance between the leading edge and the sensor is not heated.

## 3 THERMAL MASS FLOW SENSOR DESIGN

This section presents the design criteria followed for the calorimetric thermal mass flow sensor focusing on its application on air data systems. The parameters established on this section must

agree with those specified for the instrumentation circuit and manufacturing procedures, providing indications of the whole implementation cycle.

## A. Thermal mass flow sensor

The thermal mass flow sensor used in this work is the calorimetric type, where sensing elements located at opposite ends of a heater detect different temperatures due to air flow, enabling the determination of the aircraft speed. The calorimetric sensor features the capability to measure flows at low and high-speed rates with high sensitivity provided its heating temperature is kept constant [17]. Additionally, the symmetrical positioning of sensing parts allows the flow measurements in both directions. A TMFS illustration is presented in Figure 2.

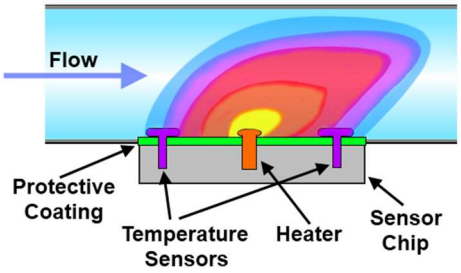


Fig. 2. Principle of operation for thermal mass flow sensor. Extracted from [18].

The calorimetric TMFS geometry is dimensioned using the heating element shaped as a serpentine with "N" loops, increasing the heated area in touch with the flow, where the metrics used for its design is presented on Figure 3.

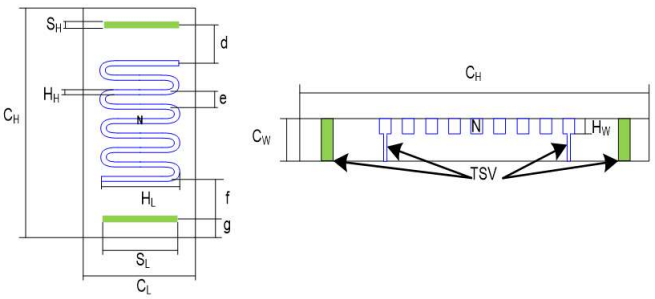


Fig. 3. Dimensions view of thermal mass flow sensor

where:

$C_H$ – Chip Height;
$C_L$ – Chip Length;
$C_W$ – Chip Width;
$H_L$ – Heater Length;
$H_W$ – Heater Width;
$H_H$ – Heater Height;
d – Distance between upstream sensing element and heater;
e – Distance between two adjacent radial portions of heater;
f – Distance between downstream sensor and heater;
g – Distance between up/downstream sensing element and edge of substrate;
$S_H$ – Sensing element Height;
$S_L$ – Sensing element Length;
$S_W$ – Sensing element Width;
N Number of radial portions of the serpentine.

To protect the TMFS contacts against the environment and keep the surface roughness as smooth as possible the Trough Silicon Via (TSV) technology will be used allowing its access in the back of the sensor.

## B. Considerations about Micro Heater

In order to ensure efficient heating transfer to air and prevent thermal leakage to the sensor elements, the micro heater was designed as a serpentine coil placed on a substrate with extremely poor thermal conductivity, depicted on sub-section D, observing the following assumptions:

The sensor is placed 10 cm away from the flat plate leading edge being not placed closed to its tips, avoiding this way any turbulence effect;

The worst-case scenario for power requirement is when the aircraft is flying at high speeds and altitudes (superior corner of aircraft operational envelope), where the fluid

temperature is the lowest and the speed is the highest possible, as presented on Table 1.

The strategy for heater design is based on calculate the required power dissipation for flow velocity measure and, consequently, the heating area and its cross-section size by using Eq. 5 which is a representation equivalent to the electrical power law $P = R \cdot I^2$. In face of these parameters, the micro heater resistance is defined in accordance also with the operational voltage available for aircraft instruments (24 V). The Table I presents the dimensions of the heater, where it conforms to the design requirements for the operation of the sensor under flight conditions. The boundary conditions for heater design are also presented.

TABLE I
HEATER DESIGN BOUNDARY CONDITIONS

| Initial Condition | VALUE |
|---|---|
| Air Temperature | -73.15 ºC |
| Flow Speed ($\mathrm{U}_\infty$) | 300 m/s |
| Prandtl Number ($\mathrm{P_r}$) | 0.737 |
| Kinematic Viscosity ($\upsilon$) | $7.59\text{x}10^{-6}$ m²/s |
| Transition Reynolds | $5\text{x}10^5$ |
| Thermal Conductivity | 0.0181 $m^{-1}$ |
| Air Density ($\rho$) | 1.7458 kg/m³ |
| Air Specific Heat | 1.007 KJ/Kg·K |
| Heater Temperature | 300 ºC |

The tungsten-based heater resistance is then dimensioned to have 32.7 Ω as presented on Table II, having its metrics defined as presented on Figure 3.

The material chosen was tungsten for providing high melting point and conformity to conventional semiconductor manufacturing process.

TABLE II
HEATER DIMENSIONS

| Dimension | VALUE |
|---|---|
| Power ($q_{conv}$) | 13.04 Watts |
| $\rho_{tungsten}$* | $3.25\text{x}10^{-8}$ Ω·m |
| d | $5\text{x}10^{-6}$ m |
| e | $2.5\text{x}10^{-5}$ m |
| f | $5\text{x}10^{-6}$ m |
| g | $5\text{x}10^{-6}$ m |
| $S_L$ and $H_L$ | $5\text{x}10^{-3}$ m |
| $H_W$ | $1\text{x}10^{-6}$ m |
| $H_H$ | $2.5\text{x}10^{-5}$ m |
| $S_W$ | $2\text{x}10^{-6}$ m |
| N | 5 |
| Resistance | 32.7 Ω |
| $x_c$** | 12,65 cm |

* This is the resistivity for the tungsten at the temperature of -73.15ºC;
** Assuming critical Reynolds number equal to $10^5$, calculated using equation (2) by isolating the term "x", at the temperature of -73.15ºC.

## C. Considerations about Sensing Elements

The distance between the up/downstream sensing elements and the micro heater is determined based on the flow velocity intended to be measured. The temperature profile is conserved or lightly displaced as the flow velocity increases. The positioning of sensing elements at a spacing distance of d=5 um may allow the sensor to operate at a desired flow speed of 300 m/s, being confirmed after CFD simulation.

The material chosen for the sensing elements relies on the transduction techniques adopted. For this application, the temperature variation is measured through metal-semiconductor junctions (Schottky diode) taking advantage of its construction simplicity [19], which is defined by a Gold and N-Type silicon junction. The junction temperature is measured as a function of the diode forward voltage variation. The manufacturing processes of these junctions are easily implemented through thin-film deposition, compatible with semiconductor technologies.

## D. Considerations about the Thermal Insulation

An ideal thermal mass flow sensor is sensitive only to the thermal effects of the fluid, measuring the convective heat. However, in real

circumstances, the conductive heat from the micro heater to the sensing element via the substrate produces an unwanted signal. Thermal insulation between the elements of the TMFS is one of the most important features to guarantee the feasibility of this type of device. Therefore, the insulating material must have very low thermal conductivity and very high electrical resistivity. The physical properties of the borosilicate glass (BSG) is suitable for this purpose. The heating element will be deposited into grooves etched over the BSG providing an adequate thermal insulation to the sensing elements. Nevertheless, the presence of upstream and downstream sensing elements provides a referential measurement signal, so that the effect of the conduction through the substrate could be reduced. Additionally, since the chosen heating material is tungsten, it is necessary to protect it against the harsh environment avoiding any damage. With that intention, the TMFS coating with a Polycrystalline Diamond thin film with outgrowing diamond (OGD) is intended. The OGD has a very high thermal conductivity and very high electrical resistivity being widely used for coating of heated elements [20].

## 4 Results

A finite-element analysis was performed using the software ANSYS Multiphysics, which can simulate structural mechanics, heat transfer, fluid flow, and the energy coupling between each of the domains.

The simulation of the thermal flow was performed in order to verify if the proposed approach will succeed in the application. The TMFS was reduced to a rectangle with an equivalent area as the heating serpentine to minimize the associated computational costs. On Figure 4(a) it is possible to see the geometrical volume with its inlet (green square) and outlet (blue square) surfaces as well as the featured heated rectangle. Figure 4(b) presents the meshing construction and how it surrounds the rectangle.

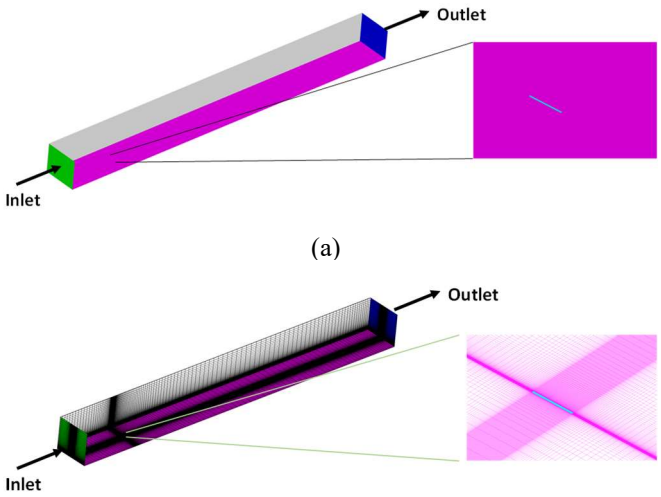


Fig. 4. (a) Heater equivalent area inside the Fairfield and (b) Meshing distribution.

Table III presents the conditions where the simulation was run. The altitude and speed was chosen seeking for the worst flying case for the TMFS operation in order to have an acceptable level of success assurance.

TABLE III
SIMULATION CONDITON

| Data | VALUE |
|---|---|
| Altitude | 45000 ft |
| Speed | 0.9 Mach (approx. 300m/s) |
| Heater Temperature | 300 ºC |
| Leading Edge Distance | 10 cm |
| Heater Area | 250µm X 5000µm |
| Meshing (number of points) | FARFIELD: 94340<br>FLAT_PLATE: 50278<br>FLUID: 5184036<br>INLET : 24453<br>OUTLET : 24453<br>SERPENTINE : 2086 |

The simulation is used to characterize the thermal profile produced by the interaction between the fluid flow and the heating element to check if the design is correct. Figure 5 presents the results obtained from the computational simulation. On Figure 5(a) it is possible to see a top view of the flow and the thermal curves. On Figure 5(b) it is presented the heat propagation on z-axis. The results present how the heat is interacting with the fluid flowing above the heating element being possible to see how far the heat is transferred and how much its temperature is dissipated. That information is the best indication about how far the downstream temperature sensor shall be

placed to avoid a big temperature drop in relation to the upstream temperature sensor. Additionally, the thermal boundary layer seems to be not disturbed by the flow, what is a good omen of success.

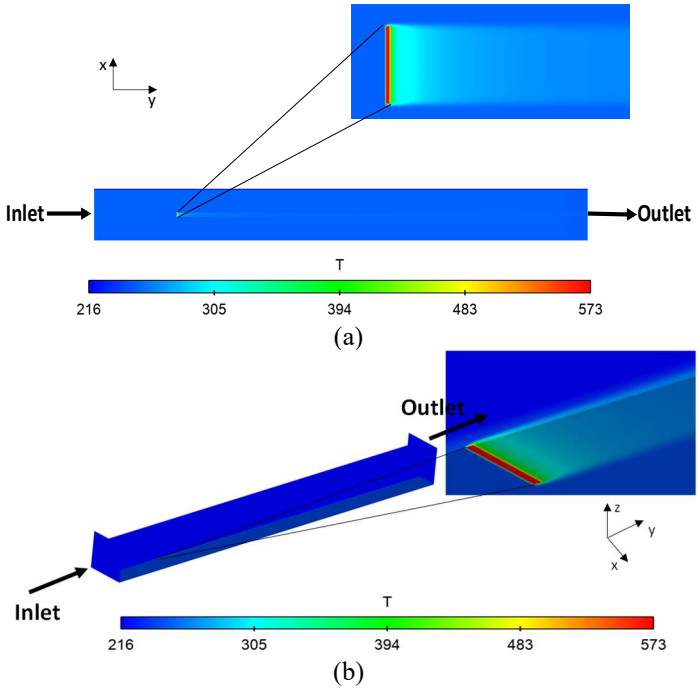


Fig. 5. (a) Heating transport over the plane (x,y) and (b) Heating transport over z axis.

## 5 Conclusion

In this paper, a thermal mass flow sensor for aeronautics application was designed presenting the criteria and rationales followed in the process. Semiconductor microfabrication processes used for the production of a TMFS establish operational adaptability for the aeronautical design needs due to: 1) its robustness and absence of moving parts; 2) capability to produce smooth surfaces disturbing as little as possible the flowing fluid; 3) easy to install and leveling; 4) high reliability rates; 5) be installed away from the flow transition point even for high flying speeds. The materials selection and the characteristics of integrant parts of the sensor define a structure of speed measurement, providing complementary measuring technology to pitot tubes.

The simulation results show that the design criteria can be considered in the construction of a mass flow sensor for aeronautical purposes. The CDF simulation results have shown the potential to succeed in the proposed application even though not modeling the TMFS elements and materials. The thermal profile generated by the interaction between the fluid flow and the heater, on Figure 5(b), appears to be placed inside the viscous sublayer, i.e. Figure 1, being not disturbed by turbulence effect originated by the surface geometry. On the other hand, the flow speed inside this region may not represent the aircraft speed and this information shall be further confirmed. Additionally, further CFD simulation presenting the thermal interaction among the TMFS elements and their materials will be executed and the results published in future work.

## 6 ACKNOWLEDGMENT

The authors would like to thanks EMBRAER for providing the computing environment to perform the simulation of this work. The authors also thank the German applied research institute Fraunhofer-ISIT and the Graduate Program on Electrical Engineering (PPGE/UFMG) for the opportunity to develop this research.

## References

[1] Nelson, R. C., “Flight Stability and Automatic Control”, McGraw-Hill Book Company, 1989. ISBN 0-07-046218-6.

[2] Haering, E. A., “Airdata Measurement and Calibration”, NASA Technical Memorandum 104316, 1995.

[3] Calia, A., Poggi, V., Schettini, F., “Air Data Failure Management in a Full-Authority Fly-By-Wire Control System”, IEEE International Conference on Control Application Proceedings, 2006.

[4] SAE Aerospace Recommended Practice, “Guidelines for Development of Civil Aircraft Systems”,SAE Standard ARP4754 Rev A, 2010.

[5] SAE Aerospace Recommended Practice, “Guidelines and Methods for Conducting the Safety Assessment Process on Civil Airborne System and Equipment”, SAE Standard ARP4761, 1996.

[6] RTCA Incorporated, “Environmental Conditions and Test Procedures for Airborne Equipment”, RTCA Standard DO-160 Rev G, 2010.

[7] Bureau d’Enquêtes et d’Analyses pour la sécurité de l’aviationcivile, “Interim Report nº2 on the accident

on 1st June 2009 to the Airbus A330-203 registered F-GZCP operated by Air France Flight AF447 Rio de Janeiro-Paris", 2009.

[8] Australian Transport Safety Bureau, "In-Flight upset 154 Km west of Learmonth, WA 7 October 2008, VH-QPA, Airbus A330-303", 2008.

[9] United Arab Emirates General Civil Aviation Authority, "Serious Incident, Unreliable Airspeed Indication, Etihad Airways, A6-EHF, Airbus A340-600", 2013.

[10] Verbeek M. J., Jentink H.W., "Optical Air Data System Flight Testing", NationaalLucht-enRuimtevaartlaboratorium, National Aerospace Laboratory NLR, 2012.

[11] Lee J.S; Yoo E.S., Park C.H., An J.E., Park C.G. and Song J.W., "Development of a Piezoresistive MEMS Pressure Sensor for a Precision Air Data Module", International Conference on Control, Automation and Systems – ICCAS, 2014.

[12] Sturm, H., Dumstorff, G., Busche, P., Westermann, D., Lang, W., "Boundary Layer Separation and Reattachment Detection on Airfoils by Thermal Flow Sensor", Sensors 2012, doi:10.3390/s121114292.

[13] UTC Aerospace Systems web site, http://utcaerospacesystems.com/cap/products/Pages/air-data-products-systems.aspx , accessed on: 01/08/2017.

[14] PRIME Faraday Partnership, "An Introduction to MEMS (Micro-electromechanical Systems)", Loughborough University, 2002. ISBN 1-84402-020-7.

[15] White, F. M., "Viscous Fluid Flow", McGraw-Hill book company, Third Edition 2006. ISBN 007-124493-X.

[16] Incropera, F. P. and Dewitt, D. P., "Fundamentals of Heat and Mass Transfer", John Wiley and Sons, 2011. ISBN 13-978-0470-50197-9.

[17] Haasl, S.; Stemme, G. Flow sensors. In Comprehensive microsystems, Gianchandani, Y.B., Tabata, O., Zappe, H., Eds.; Elsevier: Amsterdam, The Netherlands, 2008; pp. 209–272.

[18] Bapansouav, "Thermal mass flow meter (constant temperature differential)".link:https://upload.wikimedia.org/wikipedia/commons/5/53/Thermal_mass_flow_meter%28constant_temperature_differential%29.png. Accessed in 05/27/2017.

[19] Cahoon, C.; Baker, R. J. "Low-Voltage CMOS Temperature Sensor Design Using Schottky Diode-Based References", Microelectronics and Electron Devices 2008, pp. 16-19, 2008.

[20] Ullah, M.; Ahmed, E.; Elhissi, A.; Ahmed, W. "Low resistance polycrystalline diamond thin films deposited by hot filament chemical vapour deposition", Indian Academy of Sciences, Vol. 37, No. 3, May 2014.

## Copyright Issues

The content of this paper has no copyright issue to be considered in this publishing.

## Archiving

The ICAS 2018 proceedings will receive an ISBN number and will be cataloged, and archived by the German National Library.

## Copyright Statement